DIFFERENT ESTIMATION METHODS FOR TOPP-LEONE-(A) MODEL: INFERENCE AND APPLICATIONS TO COMPLETE AND CENSORED DATASETS

Adubisi O. D.[1]
Adubisi C. E.[2]
•
[1]Department of Mathematics and Statistics, Federal University Wukari, Nigeria.
[2]Department of Physics, University of Ilorin, Nigeria.

adubisiobinna@fuwukari.edu.ng[1]
chidiadubisi@gmail.com[2]

Abstract

This work proposes a new two-parameter model, titled Topp-Leone (A) model. The main benefit of the new model is that it has an inverted bathtub shaped curve, increasing and decreasing hazard rate function quite dependent on the shape parameter. Its structural properties including the ordinary moments, quantiles, probability weighted moment, median, entropy and order statistics are derived. More so, the survival, failure rate, reversed failure rate and cumulative failure rate functions are also derived. Six classical estimation methods are discussed for estimating the parameters of the new model. Monte Carlo experiments and real datasets analyses are conducted to examine the classical estimators performance of this model. Finally, the usefulness of the Topp-Leone (A) model demonstrated with different applications to complete and type-II right censored data proves its more flexible when compared to well-known models in statistical literature.

Keywords: (A)-model, Censoring, Estimation methods, Simulation, Topp-Leone-G class

1. Introduction

In the past decades, classical models have been utilized extensively for analysing various datasets in the fields of demography, engineering, finance, medical and social sciences, environmental science, biological and actuarial studies. In many workable circumstances the classical models do not give a sufficient fit to actual datasets. Therefore, various generalizations and extensions of the classical models have been proposed and studied. For example, inverse Gompertz model was pioneered by [1], odd Fréchet inverse exponential model was studied by [2], Kumaraswamy inverse Gompertz model was introduced by [3], Odd exponentiated half-logistic exponential model was studied by [4], Pareto exponential model was proposed by [5], odd exponentiated skew-t model was pioneered by [6], type-I half logistic skew-t model studied by [7], exponentiated half logistic skew-t model was introduced by [8], exponentiated odd lomax exponential model was studied by [9] and polynomial exponential model was studied by [10], among others.
[11] proposed the (A) model having just a scale parameter which makes it unsuitable for modeling most real life circumstances, hence the need to extend the (A) model to increase its flexibility and capability. The novelty and input made by this study is the creation of a new two-parameter model

known as the Topp-Leone-(A) ($TL_{(A)}$) model reliant on Eqs (3) and (4). The principal focus in this work are: utilizing the TL-G class to improve the structural properties and flexibility of the (A) model, provide a new generalized version of the (A) model with a closed-form quantile function, investigate the important descriptive aspects of the $TL_{(A)}$ model, such as the mode, median, mean, variance (VAR), skewness (SK), kurtosis (KU), moments, moment generating function, entropy, probability weighted moment and order statistics, investigate the statistical inference of the $TL_{(A)}$ model using six different methods such as the maximum likelihood estimation (MLE), maximum product spacing estimation (MPS), Anderson Darling estimation (ADE) least square estimation (LSE), and weighted least square estimation (WLSE), Cramer Von Mises estimation (CVME) for complete datasets, and provide better fits than competing generalized statistical models and also the suitability for testing the goodness of fit of the $TL_{(A)}$ to its sub-model, the (A) model.
Suppose that Z is a random variable, the cumulative distribution function (CDF) and probability density function (PDF) of the (A) model with scale parameter $\kappa > 0$ are respectively, given by

$$G(z) = e^{-\frac{1}{\kappa}\left(e^{\frac{\kappa}{z}}-1\right)};\ z > 0;\ \kappa > 0, \tag{1}$$

and

$$g(z) = \frac{1}{z^2} e^{\frac{\kappa}{z}-\frac{1}{\kappa}\left(e^{\frac{\kappa}{z}}-1\right)};\ z > 0;\ \kappa > 0. \tag{2}$$

Recently, the Topp-Leone-G (TL-G) family is one essential generator that have increased the interest of researchers in distribution theory. [12] introduced the CDF of the TL-G family as

$$F(z) = \left\{1 - [1 - G(z)]^2\right\}^{\eta}, \tag{3}$$

and the corresponding PDF to Eq (3) takes the form

$$f(z) = 2\eta g(z)\,[1 - G(z)]\left\{1 - [1 - G(z)]^2\right\}^{\eta-1}. \tag{4}$$

where $\eta > 0$ is a shape parameter, G(z) and g(z) are considered as the CDF and PDF of a baseline r.v Z.
The remaining parts are outlined as follows: Part 2 introduces the CDF and PDF of the $TL_{(A)}$ model. Part 3 presents several fundamental structural properties of the $TL_{(A)}$ model. Some essential functions used in reliability analysis are introduced in Part 4. The six classical estimation approaches are discussed in Part 5 to appreciate the parameters of the $TL_{(A)}$. The maximum likelihood estimator of $TL_{(A)}$ for the type-II right censored are presented in Part 6. The performance of $TL_{(A)}$ estimators is appreciated in Part 7 using Monte Carlo experiments. Three real datasets; two complete and one type-II right censored data are analysed and the empirical results presented in Part 8. Finally, in Part 9, discussions and conclusion are presented.

2. Topp-Leone-(A) model

2.1. Genesis of $TL_{(A)}$

The non-negative r.v Z is said to have the $TL_{(A)}$ model with parameters vector $\Psi = (\kappa, \eta)$, say Z $\sim TL_{(A)}$ (Ψ). The CDF of $TL_{(A)}$ model takes the form

$$F(z) = \left\{1 - \left[1 - e^{-\frac{1}{\kappa}\left(e^{\frac{\kappa}{z}}-1\right)}\right]^2\right\}^{\eta}, \tag{5}$$

and the corresponding PDF to Eq (5) takes the form

$$f(z) = 2\eta z^{-2} e^{\frac{\kappa}{z}-\frac{1}{\kappa}\left(e^{\frac{\kappa}{z}}-1\right)}\left[1 - e^{-\frac{1}{\kappa}\left(e^{\frac{\kappa}{z}}-1\right)}\right]\left\{1 - \left[1 - e^{-\frac{1}{\kappa}\left(e^{\frac{\kappa}{z}}-1\right)}\right]^2\right\}^{\eta-1}. \tag{6}$$

where $\eta > 0, \kappa > 0$ are the shape and scale parameters, and $z \in \Re^{+}$. Figure 1 depicts the graphical shapes of the $TL_{(A)}$ PDF with selected values for the parameters η and κ. The PDF is uni-modal, increasing-decreasing, right-skewness, decreasing, and heavy-tailed. The failure rate function of the new model in Figure 3 takes the form of "an inverted bathtub shaped, increasing and decreasing".

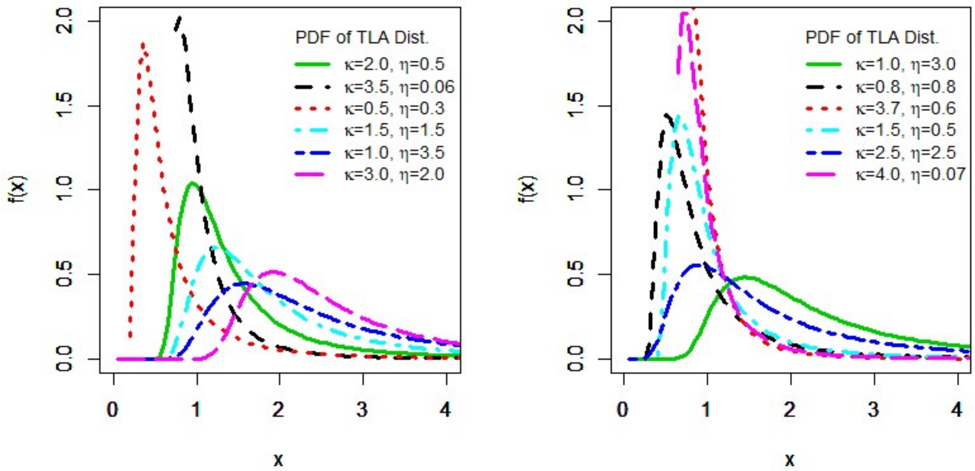

Figure 1: *The density function (PDF) plots of the $TL_{(A)}$ model.*

3. Structural properties of $TL_{(A)}$ model

This part inspects some fundamental structural properties of the $TL_{(A)}$ model.

3.1. Quantiles function

The explicit forms of the quantile and median functions for the $TL_{(A)}$ model are presented in this subpart. The quantile function found by inverting Eq (5) takes the form

$$z_u = \frac{\kappa}{\log\left\{1-\kappa\log\left[1-\left(1-u^{\frac{1}{\eta}}\right)^{\frac{1}{2}}\right]\right\}};\ 0 < u < 1, \tag{7}$$

By setting $u = \frac{1}{2}$ in Eq (7), the median (M) function takes the form

$$M = \frac{\kappa}{\log\left\{1-\kappa\log\left[1-\left(1-0.5^{\frac{1}{\eta}}\right)^{\frac{1}{2}}\right]\right\}}. \tag{8}$$

3.2. Moments and moment generating function

If $Z \sim TL_{(A)}(\Psi)$, then the r^{th} ordinary moment (OM) of Z is found using

$$\mu_r' = E\left(Z^r\right) = \int_0^\infty Z^r f\left(z;\Psi\right) dz \tag{9}$$

By substituting Eq (6) into Eq (9), expanding using the Taylor series and invoking the beta function. The OM of the $TL_{(A)}$ model takes the form

$$\mu_r' = \sum_{i=0}^{\eta-1} \vartheta_i \Gamma\left(h - r + 1\right), \tag{10}$$

where
$\vartheta_i = 2\eta \sum_{j,g=0}^{\infty} \sum_{l=0}^{g} \sum_{h=0}^{\infty} \binom{\eta-1}{i} \binom{2i+1}{j} \frac{(-1)^{g+i+j+l+1}(1+j)^g (1+g)^h \kappa^{r-g-1} l^{r-h-1}}{l! h! (g-l)!}$
Similarly, the moment generating function (MGF) of $TL_{(A)}$ model, say $M_Z(t)$ is found using

$$M_Z(t) = \mathrm{E}\left(e^{tz}\right) = \sum_{r=0}^{\infty} \frac{t^r}{r!} \int_0^{\infty} Z^r f(z;\Psi)\, dz = \sum_{r=0}^{\infty} \frac{t^r}{r!} \mu_r'. \tag{11}$$

By substituting Eq (10) into Eq (11), the MGF takes the form

$$M_Z(t) = \sum_{r=0}^{\infty} \vartheta_r \Gamma\left(h - r + 1\right), \tag{12}$$

where
$\vartheta_r = 2\eta \sum_{i=0}^{\eta-1} \sum_{j,g=0}^{\infty} \sum_{l=0}^{g} \sum_{h=0}^{\infty} \binom{\eta-1}{i} \binom{2i+1}{j} \frac{(-1)^{g+i+j+l+1}(1+j)^g (1+g)^h \kappa^{r-g-1} t^r l^{r-h-1}}{r! l! h! (g-l)!}$

3.3. Entropy measures

Entropy performs a crucial part in computer science, information theory, probability theory and engineering. It is considered as a measure of dispersion for the uncertainty associated with a random variable Z; see [13]. The Rényi entropy of Z, say $I_\tau(Z)$ is given by

$$I_\tau(Z) = \frac{1}{1-\tau} \log \int_0^{\infty} f^\tau(z)\, dz;\ \tau > 0 \text{ and } \tau \neq 1, \tag{13}$$

If $Z \sim TL_{(A)}(\Psi)$, substituting Eq (6) into Eq (13), expanding using the Taylor series and invoking the beta function. The $I_\tau(Z)$ takes the form

$$I_\tau(z) = \frac{1}{1-\tau} \log \left[\sum_{i=0}^{\tau(\eta-1)} \vartheta_i^* \Gamma\left(2i + h - 1\right) \right], \tag{14}$$

where
$\vartheta_i^* = (2\eta)^\tau \sum_{j,g=0}^{\infty} \sum_{l=0}^{g} \sum_{h=0}^{\infty} \binom{\tau(\eta-1)}{i} \binom{2i+1}{j} \frac{(-1)^{g+i+j+l+1}(\tau+j)^g (\tau+g)^h \kappa^{-2\tau-g-1} l^{-2\tau-h-1}}{l! h! (g-l)!}$

3.4. Probability weighted moment

According to [14], the probability weighted moment (PWM) is a very useful quantity in mathematical statistics. The PWM of Z, say $\zeta_{r,s}$ is given by

$$\zeta_{r,s} = \mathrm{E}\left[z^r F^s(z)\right] = \int_0^{\infty} z^r F^s(z) f(z)\, dz, \tag{15}$$

If $Z \sim TL_{(A)}(\Psi)$, substituting Eqs (5) and (6) into Eq (15), expanding using the Taylor series and invoking the beta function. The PWM $\zeta_{r,s}$ takes the form

$$\zeta_{s,r} = \sum_{a=0}^{\infty} \vartheta_a \Gamma\left(h - s + 1\right), \tag{16}$$

where
$\vartheta_a = 2\eta \sum_{b=0}^{\eta(a+1)-1} \sum_{c,i=0}^{\infty} \sum_{g=0}^{i} \sum_{h=0}^{\infty} \binom{r}{a} \binom{\eta(a+1)-1}{b} \binom{2b+1}{c}$

$\times \frac{(-1)^{b+c+i+g+1}(1+c)^i (1+i)^h \kappa^{s-i-1} g^{s-h-1}}{g! h! (i-g)!}$

3.5. Order statistics

Let $z_1, z_2, \ldots, z_n$ be a random sample from a continuous distribution, and the sequence $z_{1:n} < z_{2:n} < \ldots < z_{n:n}$ are order statistics (O.S) obtained from the sample. According to [15], he p^{th} O.S is given by

$$f_{p:N}(z) = \frac{g(z)}{\mathrm{B}(p, N-p+1)} [G(z)]^{p-1} [1 - G(z)]^{N-p}, \tag{17}$$

where $G(z)$ and $g(z)$ are the CDF and PDF of the $TL_{(A)}$ model, and $\mathrm{B}(.,.)$ is the beta function. Expanding $[1 - G(z)]^{N-p}$, the O.S takes the form

$$f_{p:N}(z) = \frac{1}{\mathrm{B}(p, N-p+1)} \sum_{l=0}^{N-p} (-1)^l \binom{N-p}{l} [F(z)]^{p+l-1} f(z), \tag{18}$$

By substituting Eqs (5) and (6) into Eq (18), and then expanding. The O.S takes the form

$$f_{p:N}(z) = \frac{2\eta}{\mathrm{B}(p, N-p+1)} \sum_{l=0}^{N-p} \frac{\vartheta_l}{z^2} e^{\frac{\kappa(1+g)}{z}}, \tag{19}$$

where
$\vartheta_l = \sum_{i=0}^{\eta(p+l)-1} \sum_{j,g=0}^{\infty} \sum_{h=0}^{g} \binom{N-p}{l} \binom{\eta(p+l)-1}{b} \binom{2i+1}{j} \frac{(-1)^{g+h+i+j+l}(1+j)^g \kappa^{-g}}{h!(g-h)!}$

3.6. Skewness, kurtosis, dispersion index and coefficient of variation

The quantile function of the $TL_{(A)}$ presented in Eq (7) can be utilized in investigating the effect of the shape parameter on the mean (ME), variance (VAR), standard deviation (STD), median (M), skewness (S_k), kurtosis (K_u), dispersion index (DI) and coefficient of variation (CV). [16] proposed the skewness computational method using the quartiles, titled Bowley skewness. It is expressed as

$$S_k = \frac{Q\left(\frac{3}{4}; \Psi\right) - 2Q\left(\frac{1}{2}; \Psi\right) + Q\left(\frac{1}{4}; \Psi\right)}{Q\left(\frac{3}{4}; \Psi\right) - Q\left(\frac{1}{4}; \Psi\right)} \tag{20}$$

Likewise, [17] introduced the kurtosis computational method based on the octiles, titled Moor's kurtosis. It is expressed as

$$K_u = \frac{Q\left(\frac{7}{8}; \Psi\right) - Q\left(\frac{5}{8}; \Psi\right) - Q\left(\frac{3}{8}; \Psi\right) + Q\left(\frac{1}{8}; \Psi\right)}{Q\left(\frac{6}{8}; \Psi\right) - Q\left(\frac{2}{8}; \Psi\right)} \tag{21}$$

The DI shows whether a model is suitable for modeling equi, under or over-dispersed datasets. More so, a distribution is considered equi-dispersed if DI = 1, under-dispersed if DI < 1 and over-dispersed if DI > 1. The DI is expressed as

$$DI = \frac{Var(X)}{E(X)} = \frac{\frac{Q\left(\frac{3}{4};\Psi\right) - Q\left(\frac{1}{4};\Psi\right)}{1.35}}{\frac{Q\left(\frac{3}{4};\Psi\right) + Q\left(\frac{1}{2};\Psi\right) + Q\left(\frac{1}{4};\Psi\right)}{3}}. \tag{22}$$

The CV is a relative measure of variability and generally utilized to compare independent samples based on their variability. A large CV value indicates a higher variability. The CV is expressed as

$$CV = \frac{(Var(X))^{\frac{1}{2}}}{E(X)} = \frac{\left(\frac{Q\left(\frac{3}{4};\Psi\right) - Q\left(\frac{1}{4};\Psi\right)}{1.35}\right)^{\frac{1}{2}}}{\frac{Q\left(\frac{3}{4};\Psi\right) + Q\left(\frac{1}{2};\Psi\right) + Q\left(\frac{1}{4};\Psi\right)}{3}}. \tag{23}$$

where $Q(.)$ is the quantile function. The numerical values of the descriptive measures for the $\text{TL}_{(\text{A})}$ model under selected values of η and κ are reported in Table 1. The following conclusions are reached:

1. The mean and standard deviation of the $\text{TL}_{(\text{A})}$ model increases as the values of κ and η increases. From the reported numerical values of the skewness and kurtosis, we can conclude that the $\text{TL}_{(\text{A})}$ model is positively skewed. Also, as the values of κ and η are increased the skewness and kurtosis values decreases.

2. The $\text{TL}_{(\text{A})}$ model is beneficial for under-dispersed datasets while the DI increases and the CV decreases, as the values of κ and η increases.

Table 1: *The descriptive measures for the $TL_{(A)}$ model.*

Parameters		Descriptive measures							
η	κ	ME	VAR	STD	M	S_k	K_u	DI	CV
0.2	0.2	0.375	0.072	0.268	0.331	0.365	1.140	0.192	0.715
0.5	0.2	0.664	0.224	0.473	0.592	0.340	1.055	0.337	0.712
1.0	0.5	1.148	0.507	0.712	1.044	0.322	0.997	0.442	0.620
2.0	0.5	1.667	1.061	1.030	1.520	0.317	0.978	0.636	0.618
2.5	1.0	2.097	1.378	1.174	1.933	0.310	0.959	0.657	0.560
3.0	1.5	2.501	1.708	1.307	2.321	0.306	0.943	0.683	0.523
3.5	1.5	2.683	1.991	1.411	2.489	0.306	0.944	0.742	0.526
3.5	2.0	2.885	2.048	1.431	2.691	0.302	0.931	0.710	0.496
4.5	2.5	3.417	2.683	1.638	3.196	0.299	0.923	0.785	0.479
5.0	3.0	3.765	3.042	1.744	3.533	0.297	0.915	0.808	0.463
6.5	3.5	4.383	3.988	1.997	4.117	0.296	0.912	0.910	0.456
7.0	4.0	4.705	4.360	2.088	4.429	0.294	0.906	0.927	0.444

Fig 2 depicts the *3D* plots of the mean, variance, skewness and kurtosis of the $\text{TL}_{(\text{A})}$ for some values of η and κ parameters. The plots in figure 2 reveal that as the values of η and κ increases, the skewness and kurtosis values decrease, and the mean and variance values increase, respectively.

4. Reliability analysis

4.1. Survival and failure rate functions

The survival function (Reliability) of $Z \sim \text{TL}_{(\text{A})}(\Psi)$, takes the form

$$R(z) = 1 - \left\{1 - \left[1 - e^{-\frac{1}{\kappa}\left(e^{\frac{\kappa}{z}}-1\right)}\right]^2\right\}^\eta ;\ \eta, \kappa > 0. \tag{24}$$

The failure (hazard) rate function (HRF) of $Z \sim \text{TL}_{(\text{A})}(\Psi)$, takes the form

$$\begin{aligned} h(z) = 2\eta z^{-2} e^{\frac{\kappa}{z} - \frac{1}{\kappa}\left(e^{\frac{\kappa}{z}}-1\right)} \left[1 - e^{-\frac{1}{\kappa}\left(e^{\frac{\kappa}{z}}-1\right)}\right] \left\{1 - \left[1 - e^{-\frac{1}{\kappa}\left(e^{\frac{\kappa}{z}}-1\right)}\right]^2\right\}^{\eta-1} \\ \times \left(1 - \left\{1 - \left[1 - e^{-\frac{1}{\kappa}\left(e^{\frac{\kappa}{z}}-1\right)}\right]^2\right\}^\eta\right)^{-1}. \end{aligned} \tag{25}$$

More so, if $Z \sim \text{TL}_{(\text{A})}(\Psi)$, then the reversed HRF takes the form

$$\begin{aligned} r(z) = 2\eta z^{-2} e^{\frac{\kappa}{z} - \frac{1}{\kappa}\left(e^{\frac{\kappa}{z}}-1\right)} \left[1 - e^{-\frac{1}{\kappa}\left(e^{\frac{\kappa}{z}}-1\right)}\right] \left\{1 - \left[1 - e^{-\frac{1}{\kappa}\left(e^{\frac{\kappa}{z}}-1\right)}\right]^2\right\}^{\eta-1} \\ \times \left(\left\{1 - \left[1 - e^{-\frac{1}{\kappa}\left(e^{\frac{\kappa}{z}}-1\right)}\right]^2\right\}^\eta\right)^{-1}. \end{aligned} \tag{26}$$

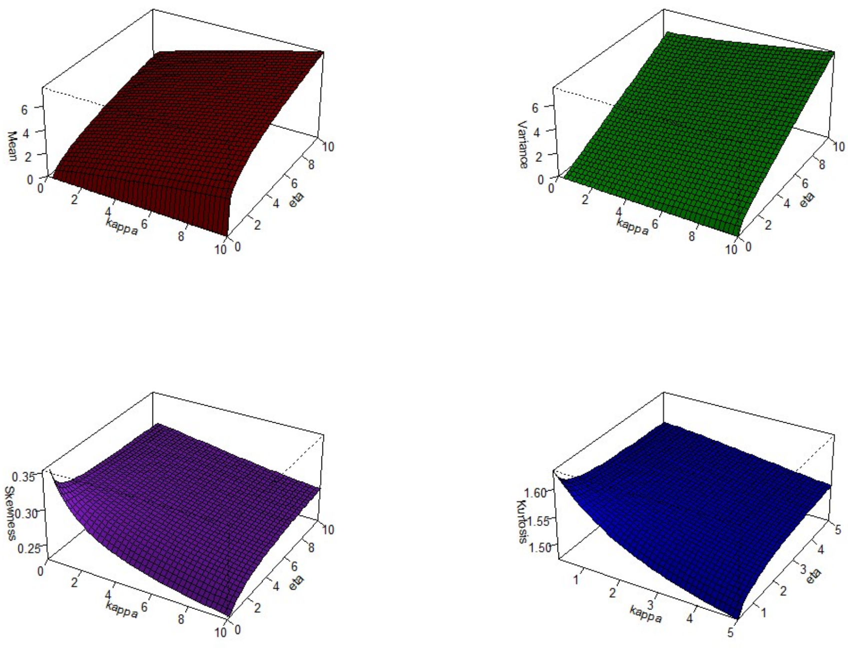

Figure 2: *The Mean, Variance, skewness and kurtosis plots of the $TL_{(A)}$ model.*

and the cumulative HRF takes the form

$$\text{H}\left(z\right) = -\log\left(1 - \left\{1 - \left[1 - e^{-\frac{1}{\kappa}\left(e^{\frac{\kappa}{z}} - 1\right)}\right]^{2}\right\}^{\eta}\right). \tag{27}$$

The graphical shapes of the HRF for $\text{TL}_{(\text{A})}$ with various selected values of η and κ are depicted in Fig 3. The model is characterized by an inverted bathtub shaped curve, increasing and decreasing HRF.

5. Estimation methods

This part discusses estimating the $\text{TL}_{(\text{A})}$ parameters via different estimation methods. The method of maximum likelihood (MLE), method of maximum product of spacing (MPS), methods of ordinary least squares (OLS) and weighted least squares (WLS), method of Cramer-Von Mises (CVM) and method of Anderson Darling (ANDA) are considered for the complete data.

5.1. The MLE

The maximum likelihood (ML) method for estimating the unknown parameters of $\text{TL}_{(\text{A})}(\Psi)$ for complete samples is considered. Let $z_1, z_2, \ldots, z_s$ be the random observed values of size (s) from $\text{TL}_{(\text{A})}(\Psi)$. Hence, the log-likelihood function $\text{L}(\Psi)$ of Eq (6) takes the form

$$\begin{aligned} L\left(\Psi\right) = {} & s\log\left(2\eta\right) + 2\sum_{j=1}^{s}\log z_j + \kappa\sum_{j=1}^{s}\frac{1}{z_j} - \frac{1}{\kappa}\sum_{j=1}^{s} v_j \\ & + \sum_{j=1}^{s}\log\left(1 - e^{-\frac{1}{\kappa}v_j}\right) + \left(\eta - 1\right)\sum_{j=1}^{s}\log\left[1 - \left(1 - e^{-\frac{1}{\kappa}v_j}\right)^{2}\right], \end{aligned} \tag{28}$$

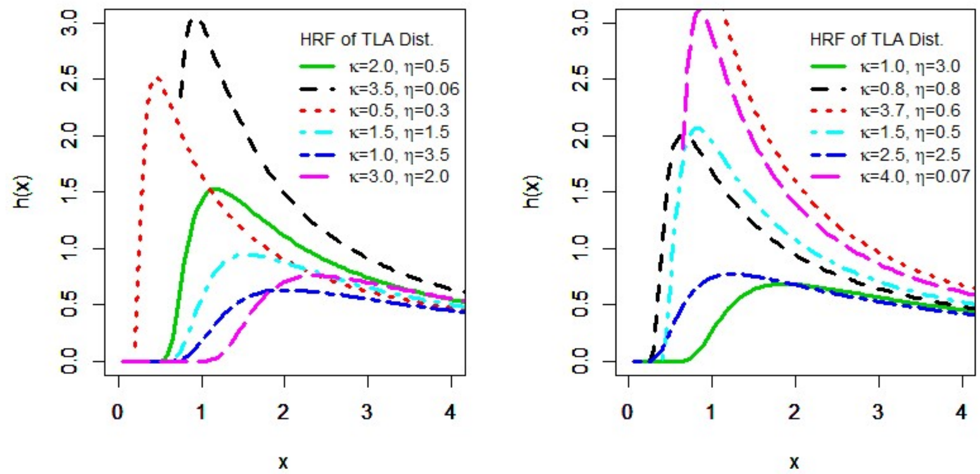

Figure 3: *The HRF plots of the $TL_{(A)}$ model.*

where $v_j = e^{\frac{\kappa}{z_j}} - 1$. By deriving the first partial derivatives of $L(\Psi)$ and equating to zero. The associated score function $U(\Psi) = \left(\frac{\partial[L(\Psi)]}{\partial\eta}, \frac{\partial[L(\Psi)]}{\partial\kappa}\right)^T = 0$ are given by

$$U_\eta(\Psi) = \frac{s}{\eta} + \sum_{j=1}^{s} \log\left[1 - \left(1 - e^{-\frac{1}{\kappa}v_j}\right)^2\right] = 0, \tag{29}$$

and

$$\begin{aligned} U_\kappa(\Psi) = {} & \sum_{j=1}^{s}\left(\frac{1}{z_j}\right) + \frac{1}{\kappa^2}\sum_{j=1}^{s}(v_j) - \frac{1}{\kappa}\sum_{j=1}^{s}\left(\frac{e^{\frac{\kappa}{z_j}}}{z_j}\right) - \sum_{j=1}^{s}(\varsigma_j) \\ & + 2(\eta-1)\sum_{j=1}^{s}\frac{\left(1-e^{-\frac{1}{\kappa}v_j}\right)\left(\frac{1}{\kappa^2}v_j - \frac{1}{\kappa z_j}e^{\frac{\kappa}{z_j}}\right)e^{-\frac{1}{\kappa}v_j}}{1-\left(1-e^{-\frac{1}{\kappa}v_j}\right)^2} = 0. \end{aligned} \tag{30}$$

where $\varsigma_j = \frac{\left(\frac{v_j}{\kappa^2} - \frac{e^{\frac{\kappa}{z_j}}}{\kappa z_j}\right)e^{-\frac{v_j}{\kappa}}}{1-e^{-\frac{v_j}{\kappa}}}$.

The ML estimates $\hat{\eta}_{\mathrm{ML}}$ and $\hat{\kappa}_{\mathrm{ML}}$ of the parameters of $\mathrm{TL}_{(\mathrm{A})}(\Psi)$ are found by maximizing Eq (**??**) using the (*Optim function*) in R-programming software.

5.2. The OLS and WLS

Let $z_{(1:s)}, z_{(2:s)}, \ldots, z_{(s:s)}$ be the ordered sample of size (s) from CDF of the $\mathrm{TL}_{(\mathrm{A})}(\Psi)$ in Eq (5). The ordinary least squares (OLS) estimates $\hat{\eta}_{\mathrm{OLS}}$ and $\hat{\kappa}_{\mathrm{OLS}}$ can be found by minimizing with respect to η and κ, the function

$$OL(\eta,\kappa) = \sum_{j=1}^{s}\left[F\left(z_{(j)}\middle|\,\eta,\kappa\right) - \xi(j,s)\right]^2, \tag{31}$$

where $\xi(j,s) = j/(s+1)$. Equivalently, the OLS estimates can be found by solving the following differential equation

$$\sum_{j=1}^{s}\left[F\left(z_{(j)}\middle|\eta,\kappa\right)-\xi(j,s)\right]\Delta_i\left(z_{(j)}\middle|\eta,\kappa\right)=0;\ i=1,2, \tag{32}$$

where

$$\Delta_1\left(z_{(j)}\middle|\eta,\kappa\right)=\frac{\partial}{\partial\eta}F\left(z_{(j)}\middle|\eta,\kappa\right),\ \Delta_2\left(z_{(j)}\middle|\eta,\kappa\right)=\frac{\partial}{\partial\kappa}F\left(z_{(j)}\middle|\eta,\kappa\right). \tag{33}$$

The solutions of Δ_i for $i=1,2$ can be found numerically. For more details, see [18].
Likewise, the weighted least squares (WLS) estimates $\hat{\eta}_{\mathrm{WLS}}$ and $\hat{\kappa}_{\mathrm{WLS}}$ can be found by minimizing with respect to η and κ, the function

$$WL(\eta,\kappa)=\sum_{j=1}^{s}\Phi(j,s)\sum_{j=1}^{s}\left[F\left(z_{(j)}\middle|\eta,\kappa\right)-\xi(j,s)\right]^2, \tag{34}$$

where $\Phi(j,s)=(s+1)^2(s+2)\Big/j(s-j+1)$. The WLS estimates can also be found by solving the following differential equation

$$\sum_{j=1}^{s}\Phi(j,s)\left[F\left(z_{(j)}\middle|\eta,\kappa\right)-\xi(j,s)\right]\Delta_i\left(z_{(j)}\middle|\eta,\kappa\right)=0;\ i=1,2, \tag{35}$$

where $\Delta_1(.\,|\eta,\kappa)$ and $\Delta_2(.\,|\eta,\kappa)$. are given in Eq (33).

5.3. The MPS

The maximum product spacing (MPS) estimator proposed by [19, 20], for the estimation of unknown parameters with ordered sample $z_{(1:s)}, z_{(2:s)}, \ldots, z_{(s:s)}$ from $\mathrm{TL}_{(\mathrm{A})}(\Psi)$, and the uniform spacing for this random sample is given by

$$D_j(\eta,\kappa)=F\left(z_{(j:s)}\,|\eta,\kappa\right)-F\left(z_{(j-1:s)}\,|\eta,\kappa\right);\ j=1,2,\ldots,T+1, \tag{36}$$

where
$F\left(z_{(0:s)}\,|\eta,\kappa\right)=0$, $F\left(z_{(s+1:s)}\,|\eta,\kappa\right)=1$.
$\sum_{j=1}^{s+1}D_j(\eta,\kappa)=1$.

The MPS estimates $\hat{\eta}_{\mathrm{MPS}}$ and $\hat{\kappa}_{\mathrm{MPS}}$ can be found by maximizing the geometric mean (GM) of the spacing given by

$$GM(\eta,\kappa)=\left[\prod_{j=1}^{s+1}D_j(\eta,\kappa)\right]^{1/s+1}, \tag{37}$$

relative to η and κ or maximizing the logarithm of GM of the spacing given by

$$LGM(\eta,\kappa)=\frac{1}{s+1}\sum_{j=1}^{s+1}\log D_j(\eta,\kappa), \tag{38}$$

The MPS estimates $\hat{\eta}_{\mathrm{MPS}}$ and $\hat{\kappa}_{\mathrm{MPS}}$ of $\mathrm{TL}_{(\mathrm{A})}(\Psi)$ can also be found by solving the following differential equation

$$\sum_{j=1}^{s+1}\frac{1}{D_j(\eta,\kappa)}\left[\Delta_i\left(z_{(j:s)}\,|\eta,\kappa\right)-\Delta_i\left(z_{(j-1:s)}\,|\eta,\kappa\right)\right]=0;\ i=1,2, \tag{39}$$

where $\Delta_1(.\,|\eta,\kappa)$ and $\Delta_2(.\,|\eta,\kappa)$ are given in Eq (33).

5.4. The ANDA

The ANDA estimates $\hat{\eta}_{\text{ANDA}}$ and $\hat{\kappa}_{\text{ANDA}}$ can be found for $TL_{(A)}(\Psi)$ by minimizing the function

$$AD(\eta,\kappa) = -s - \frac{1}{s}\sum_{j=1}^{s}(2j-1)\left[\log F\left(y_{(j:s)}\,|\eta,\kappa\right) + \log\bar{F}\left(y_{(s+1-j:s)}\,|\eta,\kappa\right)\right], \tag{40}$$

relative to η and κ. The ANDA estimates can also be found by solving the following non-linear equation

$$\sum_{j=1}^{s}(2j-1)\left[\frac{\Delta_i\left(z_{(j:s)}\,|\eta,\kappa\right)}{F\left(z_{(j:s)}\,|\eta,\kappa\right)} - \frac{\Delta_m\left(z_{(s+1-j:s)}\,|\eta,\kappa\right)}{\bar{F}\left(z_{(s+1-j:s)}\,|\eta,\kappa\right)}\right] = 0;\;\; i,m = 1,2. \tag{41}$$

where $\Delta_1(.\,|\eta,\kappa)$ and $\Delta_2(.\,|\eta,\kappa)$ are given in Eq (33).

5.5. The CVM

The CVM estimates $\hat{\eta}_{\text{CVM}}$ and $\hat{\kappa}_{\text{CVM}}$ of $TL_{(A)}(\Psi)$ are found by minimizing the function

$$CV(\eta,\kappa) = \frac{1}{12s} + \sum_{j=1}^{s}\left[F\left(z_{(j:s)}\,|\eta,\kappa\right) - \frac{2(j-1)+1}{2s}\right]^2, \tag{42}$$

relative to η and κ. Solving the non-linear equation, the CVM estimates can also be found by solving the following non-linear equation

$$\sum_{j=1}^{s}\left[F\left(z_{(j:s)}\,|\eta,\kappa\right) - \frac{2(j-1)+1}{2s}\right]\Delta_i(z_{(j:s)}\,|\eta,\kappa) = 0;\;\; i = 1,2., \tag{43}$$

where $\Delta_1(.\,|\eta,\kappa)$ and $\Delta_2(.\,|\eta,\kappa)$ are given in Eq (33).

6. MLE for type-II right censored data

Experiments on life testing is terminated when a specified number of failed objects have been observed, then the objects remaining are designated to be a type-II-right censored W. Let $z_{(1)}, z_{(2)}, \ldots, z_{(p)}$, $p \leq s$ denote the ordered values of a random sample $z_1, z_2, \ldots, z_s$ (failure times) and observations terminate after the p^{th} failure occurs, then the likelihood function (C_{t-II}) is

$$C_{t-II} = \frac{s!}{(s-p)!}\left[R\left(z_p;\Psi\right)\right]^{s-p}\prod_{j=1}^{p} f\left(z_j;\Psi\right). \tag{44}$$

If $z_1, z_2, \ldots, z_s$ is a random sample from the $TL_{(A)}(\Psi)$, then the log-likelihood function $L^{**}(\Psi)$ of $z_{(1)}, z_{(2)}, \ldots, z_{(p)}$, $p \leq s$ is

$$\begin{aligned} L^{**}(\Psi) = {} & p\log(2\eta) + \log\left(\tfrac{s!}{(s-p)!}\right) + (s-p)\log\left\{1 - \left[1 - \left(1 - e^{-\frac{2}{\kappa}v_p}\right)^2\right]^\eta\right\} \\ & -2\textstyle\sum_{j=1}^{p}\log\left(z_j\right) + \kappa\sum_{j=1}^{p}\frac{1}{z_j} - \frac{1}{\kappa}\sum_{j=1}^{p}v_j + \sum_{j=1}^{p}\log\left(1 - e^{-\frac{1}{\kappa}v_j}\right) \\ & + (\eta-1)\textstyle\sum_{j=1}^{p}\log\left[1 - \left(1 - e^{-\frac{1}{\kappa}v_j}\right)^2\right] \end{aligned} \tag{45}$$

where $v_p = e^{\frac{\kappa}{z_p}} - 1$ and $v_j = e^{\frac{\kappa}{z_j}} - 1$. The ML estimates $\hat{\eta}_{\text{ML}}$ and $\hat{\kappa}_{\text{ML}}$ of the unknown parameters of $TL_{(A)}(\Psi)$ is found by maximizing Eq (45) using the R-programming software (*Optim function*).

7. Monte Carlo experiments

In this part, the average estimates (AEs), absolute biases (AbsBs), mean square errors (MSEs) and mean relative errors (MREs) are computed for the $TL_{(A)}$ parameters (Pa.) using Monte Carlo experiments with complete samples.

7.1. Monte Carlo experiments based on complete data

These Monte Carlo experiments are executed in R-programming software and the sampling distributions are found for different sample sizes (T) from s = 3000 replications for various values of κ and η. The classical estimators discussed in Part 5 for complete data are assessed and the average estimates (AEs) for each estimator are presented in Tables 2, 3 and 4. The comparison of the estimators graphically according to the AbsBs, MSEs and MREs for the $TL_{(A)}$ parameters (Pa.) are depicted in Figures 4, 5 and 6. Therefore, the following conclusions are reached utilizing the graphical plots.

1. The estimators are asymptotically unbiased given that their absolute biases converge to zero as the sample size increases. The estimators are consistent given that their MSEs tend to zero for large sample size.
2. The MLE and OLS performs better than the other estimators in terms of minimum AbsBs and MREs in most cases while the MPS has the largest absolute biases and MREs compared to other estimators in most cases. The results indicate that the MLE, OLS, WLS, ANDA, CVM and MPS perform quite well in estimating the $TL_{(A)}$ model parameters.

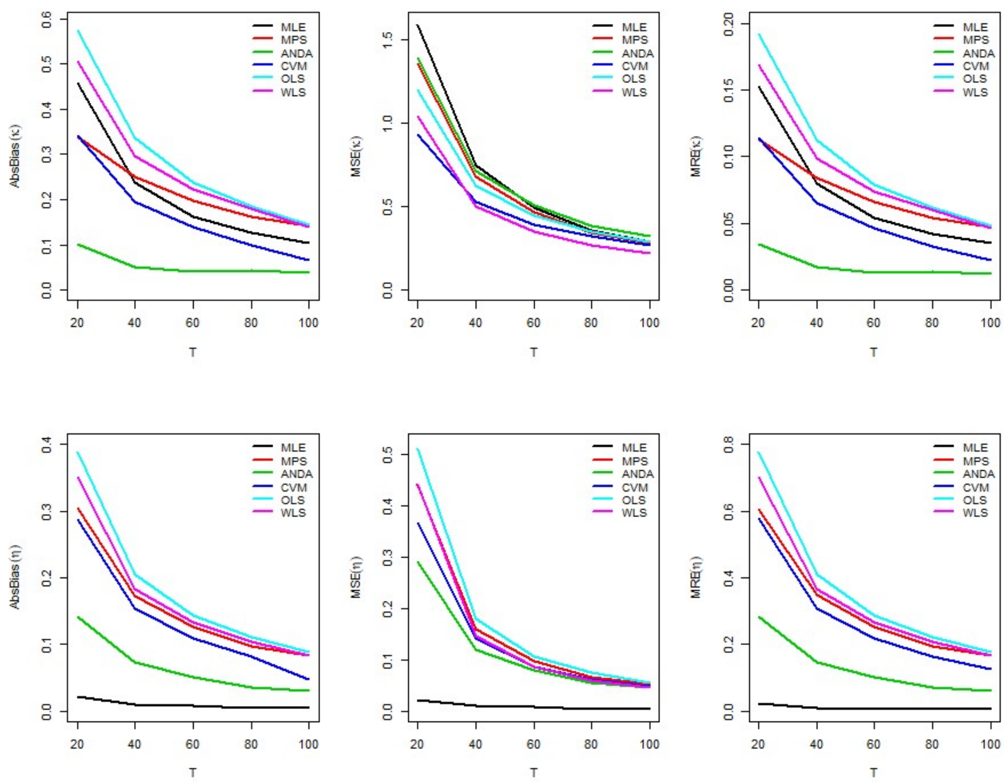

Figure 4: *The estimators AbsBs, MSEs and MREs when $\kappa = 3.0$ and $\eta = 0.5$ (complete data).*

Table 2: *The estimators AEs when $\kappa = 3.0$ and $\eta = 0.5$ based on complete data.*

T	Pa.	MLE	OLS	WLS	MPS	ANDA	CVM
20	κ	3.458	2.425	2.493	2.662	3.102	2.659
	η	0.522	0.889	0.850	0.804	0.642	0.788
40	κ	3.239	2.664	2.704	2.749	3.051	2.805
	η	0.510	0.705	0.683	0.673	0.573	0.653
60	κ	3.163	2.763	2.777	2.802	3.040	2.862
	η	0.507	0.643	0.633	0.626	0.551	0.609
80	κ	3.127	2.815	2.820	2.837	3.042	2.901
	η	0.504	0.611	0.604	0.597	0.535	0.582
100	κ	3.104	2.855	2.861	2.859	3.037	2.933
	η	0.504	0.588	0.583	0.583	0.530	0.563

Table 3: *The estimators AEs when $\kappa = 3.5$ and $\eta = 2.0$ based on complete data.*

T	Pa.	MLE	OLS	WLS	MPS	ANDA	CVM
50	κ	3.788	3.491	3.562	3.220	3.610	3.750
	η	2.003	2.286	2.200	2.460	2.161	2.100
100	κ	3.649	3.528	3.572	3.320	3.568	3.660
	η	2.004	2.134	2.080	2.270	2.081	2.040
150	κ	3.598	3.516	3.552	3.360	3.545	3.600
	η	2.005	2.091	2.051	2.190	2.056	2.030
200	κ	3.577	3.513	3.542	3.380	3.536	3.580
	η	1.999	2.064	2.033	2.150	2.037	2.020
250	κ	3.562	3.514	3.538	3.400	3.531	3.570
	η	2.000	2.051	2.025	2.120	2.030	2.010

Table 4: *The estimators AEs when $\kappa = 2.0$ and $\eta = 2.5$ based on complete data.*

T	Pa.	MLE	OLS	WLS	MPS	ANDA	CVM
200	κ	2.056	2.006	2.029	1.920	2.023	2.060
	η	2.492	2.562	2.530	2.650	2.536	2.510
400	κ	2.025	2.002	2.015	1.950	2.010	2.030
	η	2.502	2.535	2.517	2.590	2.522	2.510
600	κ	2.013	2.000	2.008	1.950	2.004	2.020
	η	2.506	2.526	2.515	2.570	2.518	2.510
800	κ	2.009	1.999	2.005	1960	2.002	2.010
	η	2.504	2.521	2.511	2.550	2.514	2.510
1000	κ	2.008	2.000	2.005	1.970	2.003	2.010
	η	2.502	2.514	2.507	2.540	2.509	2.500

8. Data applications

The flexibility of the $TL_{(A)}$ model is demonstrated here with three real datasets; two complete data and one type-II right censored data.

8.1. Applications for complete data

The first dataset corresponding to the relief times of twenty patients receiving an analgesic was previously analysed by [22]. 1.1, 1.4, 1.3, 1.7, 1.9, 1.8, 1.6, 2.2, 1.7, 2.7,4.1, 1.8, 1.5, 1.2, 1.4, 3.0, 1.7, 2.3, 1.6, 2.0. The second dataset corresponding to the scores of the general rating of affective symptoms for preschoolers (GRASP) which measures the emotional and behavioural problems of children was previously analysed by [1] and [11]. 19(16), 20(15), 21(14), 22(9), 23(12), 24(10), 25(6), 26(9), 27(8), 28(5), 29(6), 30(4), 31(3), 32(4), 33(1), 34(1), 35(4), 36(2), 37(2), 39(1), 42(1), 44(1). The MLE will be used to compare the goodness-of-fit of the $TL_{(A)}$ with the (A) model, inverse Gompertz (IG) model, lomax(LOMX) model, Pareto (PE) model, inverse Pareto (IPE) model, Pareto type-I (PETI) model, exponentiated inverse rayleigh (EIR) model, type-I half logistic skew-t (TIHLST) model, generalized inverse exponential (GIE) model and odd frechet inverse exponential

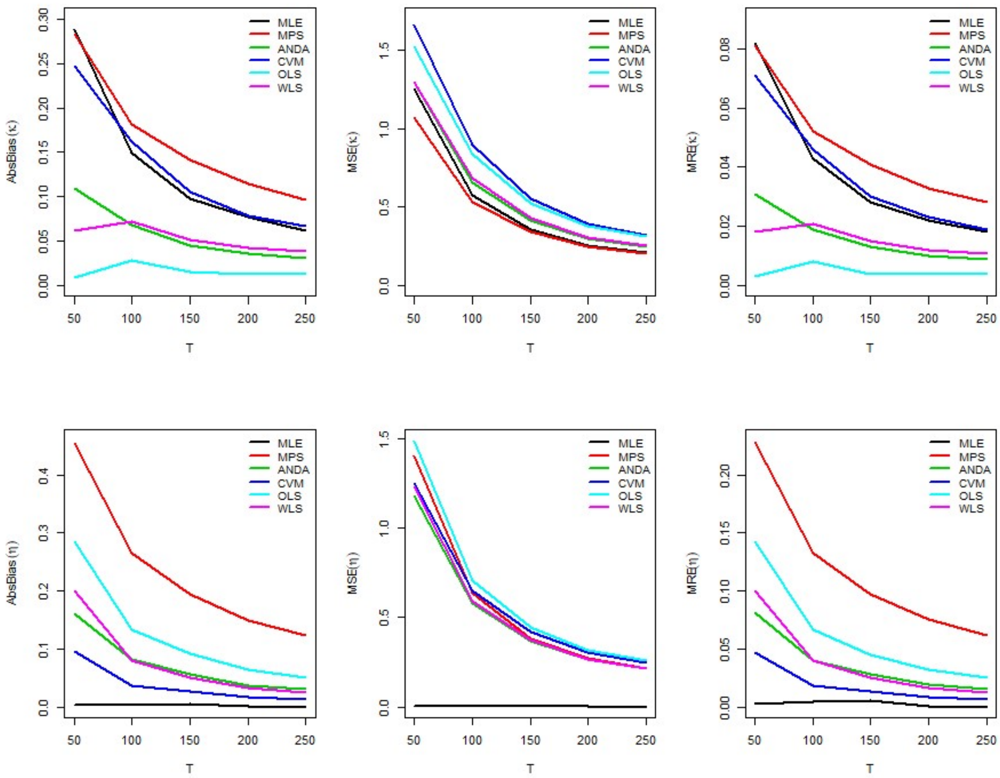

Figure 5: *The estimators AbsBs, MSEs and MREs when* $\kappa = 3.5$ *and* $\eta = 2.0$ *(complete data).*

(OFIE) model. These models will be fitted to the two complete datasets according to some criteria, namely, the Kolmogorov Smirnov test statistic (K.S) with its PVs. The Akaike information criterion (AIC), correct Akaike information criterion (CAIC), Hannan-Quinn information criterion (HQIC), Bayesian information criterion (BIC), Cramér-von Mises (W) statistic, Anderson-Darling (A) statistic and log-likelihood value (LL) will also be provided. The analysis is performed with the R-programming software using the *fitdistrplus*, *Optim* and *AdequacyModel packages*.

First dataset analysis

The MLEs, K.S and PVs for the first dataset are provided in Table 5 for all the studied models. The results show that the TL$_{(A)}$ has the least values for LL, AIC, CAIC, HQIC, BIC, and KS value with largest PV. This highlights that the TL$_{(A)}$ fits the first dataset better than (A), IG, LOMX, PE, IPE, PETI, OFIE, EIR, TIHLST and GIE models. This confirms that the TL$_{(A)}$ seems to be a very good model better than the other competing models. More so, the TL$_{(A)}$ model gives a more appropriate fit to the first data than the Kumaraswamy-transmuted exponentiated modified Weibull (KwTEXMW), McDonald log-logistic (McDLL), beta Weibull (BWE), modified Weibull (MWE), transmuted complementary Weibull geometric (TCWEG) and exponentiated transmuted generalized Rayleigh (ETGRH) models (see Table 5, [22]). Figure 7 depicts the fitted PDFs and fitted CDFs of all the models. The plots support the results presented in Table 5 that the TL$_{(A)}$ model provides the best goodness of fits to the first dataset.

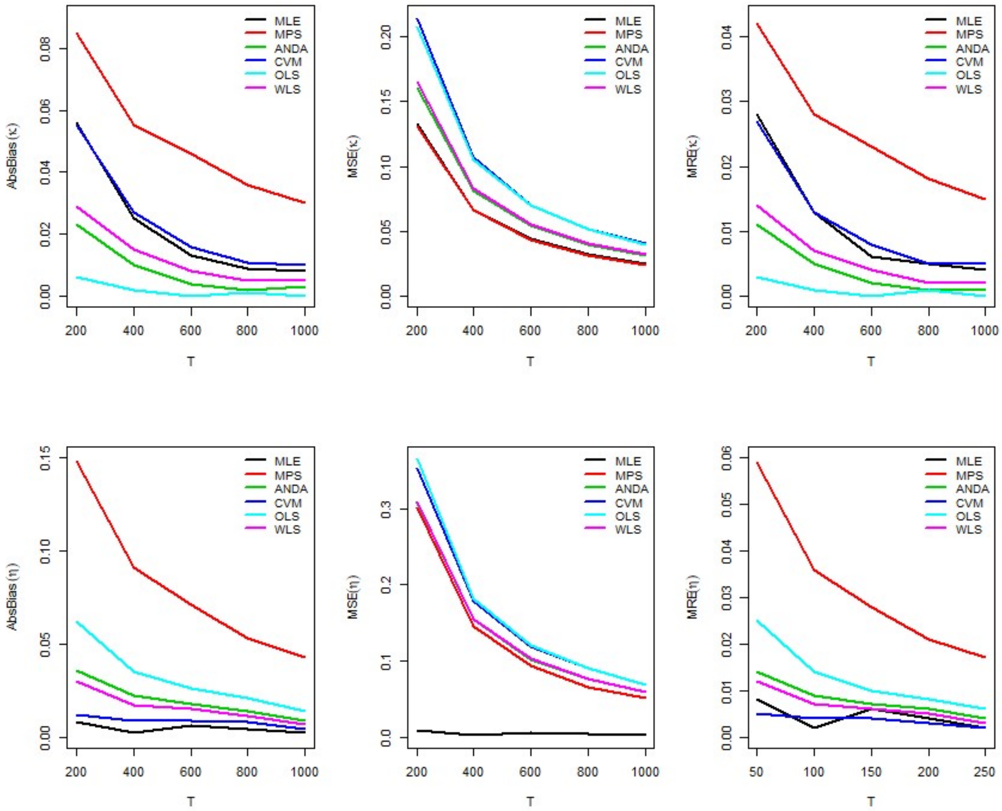

Figure 6: *The estimators AbsBs, MSEs and MREs when $\kappa = 2.0$ and $\eta = 2.5$ (complete data).*

Table 5: *The MLEs, KS, PVs, LL, AIC, BIC, CAIC, HQIC, W* and A* values for the first dataset.*

	Models										
	TLA	A	IG	LOMX	PE	IPE	PETI	GIE	TIHLST	EIR	OFIE
$\hat{\kappa}$	5.092	2.402	6.145	28.385	25.011	28.862	1.697	36.485	0.708	3.610	1.329
$\hat{\eta}$	0.228	-	0.110	0.019	47.333	0.059	-	2.232	2.347	2.336	0.906
K.S	0.116	0.385	0.142	0.444	0.437	0.380	0.285	0.134	0.504	0.127	0.358
PV	0.952	0.005	0.812	0.001	0.001	0.006	0.078	0.862	7.6E-05	0.906	0.012
LL	-15.650	-23.503	-16.392	-33.142	-33.182	-32.986	-21.207	-16.261	-38.265	-15.868	-26.591
AIC	35.300	49.006	36.783	70.283	70.364	69.972	44.414	36.521	80.529	35.736	57.181
CAIC	36.005	49.229	37.489	70.989	71.070	70.678	44.636	37.227	81.235	36.442	57.887
BIC	37.291	50.002	38.774	72.275	72.356	71.963	45.410	38.513	82.520	37.727	59.172
HQIC	35.688	49.201	37.172	70.672	70.729	70.361	44.609	36.910	80.918	36.125	57.570
W*	0.025	0.028	0.055	0.102	0.102	0.050	0.038	0.054	0.090	0.042	0.032
A*	0.105	0.162	0.332	0.607	0.605	0.293	0.219	0.319	0.533	0.244	0.179

Second dataset analysis

The MLEs, KS and PVs for the second dataset are provided in Table6 for all studied models. The results show that the $TL_{(A)}$ has the least values for LL, AIC, CAIC, HQIC, BIC, and KS value with largest PV. This highlights that the $TL_{(A)}$ fits the second dataset better than (A), IG, LOMX, PE, IPE, PETI, OFIE, EIR, TIHLST and GIE models. This confirms that the $TL_{(A)}$ seems to be a very good model better than the other competing models. More so, the $TL_{(A)}$ model gives a more appropriate fit to the second data than the generalized exponential (GEX), Gompertz (GTz), extended Gompertz (EGTz) and generalized Gompertz (GGTz) models (see Table 5, [1]). Figure 8 depicts the fitted pdfs and fitted CDFs plots of all the models. The plots support the results

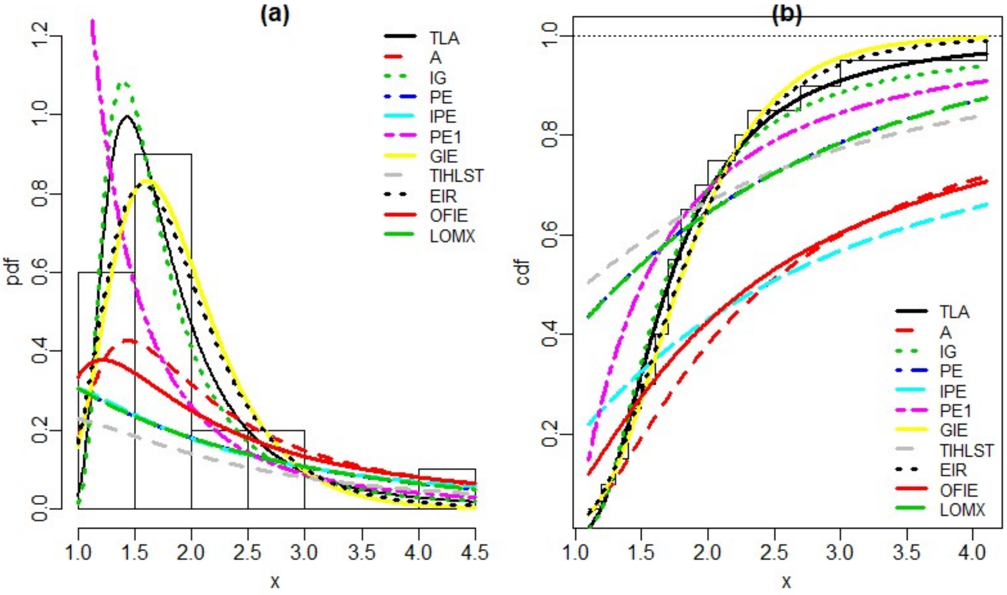

Figure 7: *Fitted density function (pdf) plot (left panel), Fitted distribution function (CDF) plot (right panel) for the $TL_{(A)}$ model (first dataset).*

presented in Table 6 that the $TL_{(A)}$ model provides the best goodness of fits to the second dataset.

Table 6: *The MLEs, KS, PVs, LL, AIC, BIC, CAIC, HQIC, W* and A* values for the second dataset.*

	Models										
	TLA	A	IG	LOMX	PE	IPE	PETI	GIE	TIHLST	EIR	OFIE
$\hat{\kappa}$	86.970	107.354	149.337	3.328	7.808	63.123	0.313	138.914	0.676	10.246	18.987
$\hat{\eta}$	4.809	-	0.175	0.012	185.974	0.379	-	0.218	359.391	40.286	0.943
K.S	0.100	0.130	0.102	0.495	0.532	0.452	0.602	0.108	0.572	0.109	0.446
PV	0.138	0.022	0.120	2.2E-16	2.2E-16	2.2E-16	2.2E-16	0.088	2.2E-16	0.085	2.2E-16
LL	-393.202	-404.277	-393.401	-582.812	-573.127	-565.908	-718.074	-399.265	-601.745	-401.694	-520.798
AIC	790.404	810.555	790.801	1169.625	1150.253	1135.816	1438.148	802.530	1207.490	807.388	1045.595
CAIC	790.496	810.585	790.893	1169.716	1150.345	1135.907	1438.179	802.622	1207.582	807.479	1045.687
BIC	796.200	813.453	796.597	1175.420	1156.049	1141.611	1441.046	808.326	1213.286	813.452	1051.391
HQIC	792.759	811.732	793.157	1171.980	1152.608	1138.171	1439.326	804.886	1209.846	809.743	1047.951
W	0.208	0.209	0.235	0.371	0.388	0.286	0.302	0.246	0.377	0.322	0.227
A	1.523	1.525	1.708	2.512	2.613	1.994	2.091	1.756	2.545	2.214	1.631

For the $TL_{(A)}$, the approximate 95% two-sided confidence intervals (CIs) for the parameters κ and η are $[2.276, 7.909]$ and $[-0.176, 0.632]$ for the first dataset and $[65.743, 108.197]$ and $[-1.249, 10.868]$ for the second dataset, respectively. The likelihood ratio test (LRT) is normally used to test if the fit by $TL_{(A)}$ model is statistically superior to the fit provided by the (A) model. Table 7 provides the values of the LRT, degree of freedom (d.f) and its PVs for the first and second datasets. Based on the PVs, the null hypothesis (H_0) is rejected at $\alpha = 0.05$ level of significance.

Table 7: The LR tests for the first and second datasets.

Model	Hypotheses	LR	PV
	First dataset		
(A) vs. $TL_{(A)}$	$H_0 : \eta = 1$ *vs.* $H_1 : H_0$ *is false*	15.707	0.00074
	Second dataset		
(A) vs. $TL_{(A)}$	$H_0 : \eta = 1$ *vs.* $H_1 : H_0$ *is false*	22.151	0.0000025

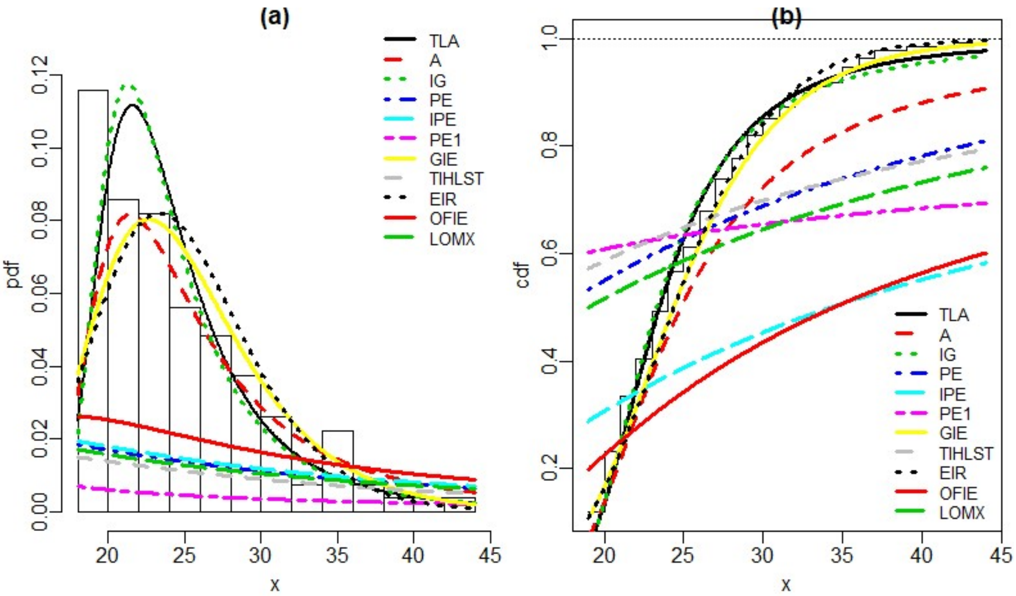

Figure 8: *Fitted density function (pdf) plot (left panel), Fitted distribution function (CDF) plot (right panel) for the $TL_{(A)}$ model (second dataset).*

8.2. Application for censored data

The censored data used here which represents the fatigue life for 10 bearings of a specific type in hours was introduced by DD. 152.7, 172, 172.5, 173.5, 193, 204.7, 216.5, 234.9, 262.6, 422.6. Assume a type II right censored sample of size $p = 8$ is taken from this data. Table 8 shows the MLEs, LL, K.S and PV for the $TL_{(A)}$ model. It is clear that the $TL_{(A)}$ well fitted to the data based on the K.S and its PV.

Table 8: *The MLEs and performance measures for the type-II right censored data.*

Models	MLEs	LL	K.S	PV
$TL_{(A)}$	$\kappa = 539.86,\ \eta = 946.82$	-41.129	0.263	0.550

9. Discussions and Conclusion

In this work, a new model titled $TL_{(A)}$ which is considered as an extension and generalization to the (A) model is proposed. The $TL_{(A)}$ is characterized by an inverted bathtub shaped curve, increasing and decreasing hazard rate function quite dependent on the shape parameter. More so, the $TL_{(A)}$ is appropriate for testing the goodness of fit of the sub-model, the (A) model. Some structural properties including the ordinary and incomplete moments, MGFs, PWMs, quantiles, Bonferroni and Lorenz curves, entropies, median and order statistics of $TL_{(A)}$ are derived. Likewise, basic functions utilized in reliability theory such as the survival function, HRF, reversed HRF, cumulative HRF, MTTF, MRL and MWT are derived. The Monte Carlo experiments are carried out to determine the performance of MLE, MPS, ANDA, CVM, OLS and WLS methods according to AbsBs, MSEs and MREs measures. The experiments results indicate that the estimators perform quite well in producing good parameter estimates for all the various parameter groups at different sample sizes. However, the MLE method produced closer estimates for $TL_{(A)}$ parameters. This conforms to the reports by [24, 25, 26, 27, 28]. Furthermore, the parameters of $TL_{(A)}$ are appreciated using the MLE in the case of complete and type-II-right censored data. The two complete data are analysed using the $TL_{(A)}$ and compared with ten other competing lifetime models. Likewise, a type-II-right censored data is analysed using the $TL_{(A)}$ model. The results indicate that the $TL_{(A)}$ has more flexibility for fitting the various datasets.

Futuristically, the bivariate extension of the $TL_{(A)}$ model, the $TL_{(A)}$–G family of distributions and the discrete case of the $TL_{(A)}$ model will be addressed.

References

[1] Eliwa, M. S., El-Morshedy, M and Ibrahim, M. (2009). Inverse Gompertz distribution: properties and different estimation methods with application to complete and censored data. *Annals of data science*, 6(2):321–339.

[2] Alrajhi, S. (2019). The odd Fréchet inverse exponential distribution with application. *Journal of Nonlinear Sciences & Applications (JNSA)*, 12(8):1–24.

[3] El-Morshedy, M., El-Faheem, A. A. and El-Dawoody, M. (2020). Kumaraswamy inverse Gompertz distribution: Properties and engineering applications to complete, type-II right censored and upper record data. *Plos one*, 15(12):e0241970.

[4] Aldahlan, Maha, A. D. and Afify, A. Z. (2020). The odd exponentiated half-logistic exponential distribution: estimation methods and application to engineering data. *Mathematics*, 8(10):1684.

[5] Rana, M. S. and Rahman, M. M. (2022). The Pareto-Exponential Distribution: Theory and Real-life Applications.*European Journal of Mathematics and Statistics*, 3(3):30–39.

[6] Adubisi, O. D., Abdulkadir, A. and Chiroma, H. (2021). A Two Parameter Odd Exponentiated Skew-T Distribution With J-Shaped Hazard Rate Function. *Journal of Statistical Modeling & Analytics (JOSMA)*, 3(1): 26–46.

[7] Adubisi, O. D., Abdulkadir, A., Chiroma, H. and Abbas, U. F. (2021). The type I half logistic skew-t distribution: A heavy-tail model with inverted bathtub shaped hazard rate. *Asian J Probab Stat*, 14:21–40.

[8] Adubisi, O. D., Abdulkadir, A., Abbas, U. F. and Chiroma, H. (2021). Financial data and a new generalization of the skew-t distribution.*Covenant Journal of Physical and Life Sciences*, 9(2):1–17.

[9] Dhungana, G. P. and Kumar, V. (2022). Exponentiated Odd Lomax Exponential distribution with application to COVID-19 death cases of Nepal. *PloS one*, 17(6):e0269450.

[10] Beghriche, A., Zeghdoudi, H., Raman, V. and Chouia, S. (2022). New polynomial exponential distribution: properties and applications. *Statistics in Transition new series*, 23(3):95–112.

[11] Alshenawy, R. (2020). A new one parameter distribution: properties and estimation with applications to complete and type II censored data. *Journal of Taibah University for Science*, 14(1):11–18.

[12] Al-Shomrani, A., Arif, O., Shawky, A. Hanif, S. and Shahbaz, M. Q. (2016). Topp–Leone family of distributions: Some properties and application. *Pakistan Journal of Statistics and Operation Research*, 7:443–451.

[13] Rényi, A. (1961). Proceedings of the Fourth Berkeley Symposium on Mathematical Statistics and Probability. *Contributions to Biology and Problems of Medicine*, 4:547-561.

[14] Greenwood, J. A., Landwehr, J. M., Matalas, N. C and Wallis, J. R. (1979). Probability weighted moments: definition and relation to parameters of several distributions expressable in inverse form. *Water resources research*, 15(5):1049-1054.

[15] David, H. A. and Nagaraja, H. N. Order statistics, John Wiley & Sons, 2004.

[16] Kenney, J. F. Mathematics of statistics, D. Van Nostrand, 1939.

[17] Moors, J. J. A. (1988). A quantile alternative for kurtosis. *Journal of the Royal Statistical Society: Series D (The Statistician)*, 37(1):25–32.

[18] Swain, J. J., Venkatraman, S. and Wilson, J. R. (1988). Least-squares estimation of distribution functions in Johnson's translation system. *Journal of Statistical Computation and Simulation*, 29(4):271–297.

[19] Cheng, R. C. H and Amin, N. A. K. (1979). Maximum product-of-spacings estimation with applications to the lognormal distribution. *Math report*, 791.

[20] Cheng, R. C. H and Amin, N. A. K. (1983). Estimating parameters in continuous univariate distributions with a shifted origin. *Journal of the Royal Statistical Society: Series B (Methodological)*, 45(3):394–403.

[21] Zheng, G. and Park, S. (2004). On the Fisher information in multiply censored and progressively censored data. *Communications in Statistics-Theory and Methods*, 33(8):1821–1835.

[22] Afify, A., Yousof, H. and Nadarajah, S. (2017). The beta transmuted-H family for lifetime data. *Statistics and its Interface*, 10(3):505–520.

[23] McCool, J. I. (1978). Competing risk and multiple comparison analysis for bearing fatigue tests. *ASLE transactions*, 21(4):271–284.

[24] Ramos, P. L., Louzada, F., Ramos, E. and Dey, S. (2020). The Fréchet distribution: Estimation and application-An overview. *Journal of Statistics and Management Systems*, 23(3):549-578.

[25] Chesneau, C., Bakouch, H. S., Ramos, P. L. and Louzada, F. (2020). The polynomial-exponential distribution: A continuous probability model allowing for occurrence of zero values. *Communications in Statistics-Simulation and Computation*, 22:1–26.

[26] Adubisi, O. D., Abdulkadir, A. and Adashu, D. J. (2022). Improved Parameter Estimators for the Flexible Extended Skew-t Model with Extensive Simulations, Applications and Volatility modeling. *Scientific African*, e01443.

[27] Adubisi, O. D., Adubisi, C. E. and Abdulkadir, A. (2022). Laplace Transformed Properties of the Extended Power-Gompertz Model: Simulation and Applications. *Scientific African*, e01523.

[28] Adubisi, O. D., Abdulkadir, A. and Adubisi, C. E. (2022). A new hybrid form of the skew-t distribution: estimation methods comparison via Monte Carlo simulation and GARCH model application. *Data Science in Finance and Economics*, 2(2):54-79.